

NOVABOT: a mini-blimp dedicated to stage recording

Second year internship report by:

Mateo de Jesus Cortés
2A Electronics Engineering

15 May 2023 - 8 September 2023



©Youssra MANSAR - Le Festival Printemps, Aix-en-Provence

Supervisors:

Julien SERRES (MCU-HDR ISM - AMU)
François BERNIER (Engineer ID-Fab - EMSE)

Tutor ENSEA:

Roseline Descout-Renier

Contents

1 Abstract	1
2 Introduction	2
3 State of the Art	3
3.1 The mini blimps	3
3.1.1 Similar projects	3
3.1.2 Related works	7
4 Research groups involved in NOVABOT	10
4.1 ISM (Institut des Sciences du Mouvement)	10
4.2 LESA (Laboratoire d'Etude en Science des Arts)	12
4.3 ID-Fab - École des Mines de Saint-Étienne	12
5 State of the art in mini airships	13
5.1 Functions of ID-Fly airship	14
5.2 Envelope and structure	14
5.3 Mass balance and forces exerted	16
5.4 Embedded Electronics	18
6 Progress made in the internship	19
6.1 Camera	19
6.2 Dynamic modeling of ID-Fly airship	21
6.3 Autonomous system	24
6.3.1 Goals for the autonomous System	24
6.3.2 Measurement of thrusters	24
6.3.3 Control algorithm	25
6.4 Simulation	29
7 Further steps and solutions	30
8 Conclusion	30
9 Acronyms	32
References	33
Annexes	36

LIST OF FIGURES

List of Figures

1	Mini-Blimp, from Zufferey et al. [34].	4
2	Mini blimp basket from Zhang [32].	5
3	Mini-blimp 3D printing basket [8].	6
4	Possible positions for the basket [8]: centered (a) and eccentric (b). In the end, configuration (b) was chosen.	6
5	Mini blimp basket from Gonzalez et al. [7].	7
6	Diagram of airship from Ikeda et al. [12].	7
7	How a micro blower works [12].	8
8	First version of Georgia Tech Miniature Autonomous Blimp (GT-MAB) by Georgia Tech, USA [23].	8
9	Mini-blimps Basket GT-MAB [30]	9
10	Fin-propelled airship [18]	9
11	Organisation chart of the Institut des Sciences du Mouvement - Etienne-Jules Marey (CNRS/Aix Marseille Université, Institut des Sciences du Mouvement - Etienne-Jules Marey (CNRS/Aix Marseille Université, ISM UMR7287) (ISM) UMR7287). Source : https://ism.univ-amu.fr/fr/l'institut/organigramme	11
12	Innovation, Fabrication-Design (ID-Fab) functioning. Source: https://www.mines-stetienne.fr/recherche/plateformes/id-fab/	13
13	User Interface for backstage.	14
14	Envelope of the ID-Fly blimp.	15
15	Diagram of the mini-blimp ID-Fly.	16
16	New battery with mounting parts.	16
17	Balance of forces applied to the steering system.	17
18	Balance of the airship's useful mass. From [21].	18
19	Raspberry Pi Zero W with a converter, shield, drivers, and camera. From [21].	19
20	Caméra Luxonis OAK-D-IoT-40. Size: 60mm large, height 45mm, large 25mm; mass: 45g in technical documentation.	20
21	Blimp axis and angles.	21
22	Free body diagram of the ID-Fly blimp.	22
23	CAD Model	23
24	Kinovea Simulation	24
25	Thrusters measurement test bench.	25
26	Thrusters gain.	25
27	Distance error over time with control by controller Proportional Integral Derivative (PID).	28
28	Course error over time with aPID controller.	28
29	Simulation scene in v-rep.	29
30	Simulation communication with Robot Operating System (ROS).	30
31	Caption	37

1 ABSTRACT

Acknowledgments

I would like to extend my heartfelt gratitude to Dr. Julien Serres and Mr. Francois Bernier for granting me the invaluable opportunity to contribute to the NOVABOT project. Your guidance and unwavering patience throughout the process have been instrumental in my growth and learning. A special thank you to Youssra Mansar for introducing me to this field, laying the foundation for my journey.

I am also deeply appreciative of the support provided by Valentin Divay, PhD student. Your assistance and availability, stemming from your extensive experience in the earlier phases of the project, proved to be incredibly beneficial.

I also express my gratitude to my colleague Thibault Langlart, a fellow intern from the École Nationale Supérieure de Techniques Avancées Bretagne (ENSTA Bretagne), in his third year. Your collaboration and support during every stage of my internship have been invaluable.

Lastly, I extend my thanks to Mister Eneko Chipy, the ENSEA's international relations director. Your assistance in managing logistics before and during the internship has been of immense help.

1 Abstract

During a second-year internship at the Georges Charpak Provence campus of Mines Saint-Étienne, located in Gardanne, Provence, I collaborated with a final-year master's engineering student, Thibault Langlart, within the Novabot project. This project aimed to integrate a floating drone called the "ID-FLY airship" into theatrical applications to provide a unique perspective of performance scenes. Working at the ID-Fab facility under the supervision of research engineer Francois Bernier and Dr. Julien Serres, we focused on automating the drone's behavior to maintain a fixed distance from artists on stage. Our tasks included implementing the ROS framework on a Raspberry Pi, adapting the Luxonis AI camera as a position sensor, creating a dynamic model, and developing the flight control system. Additionally, we contributed to an artistic demonstration led by Ph.D. student Youssra Mansar, who is conducting artistic research as part of her thesis at LESA in Aix-en-Provence.

Keywords : coding, flight control systems, blimps, electronics, micromechanics, theater, robotics.

2 Introduction

During my second-year internship, I was stationed at the Georges Charpak Provence campus of the Engineering school *Mines Saint-Étienne*, situated in Gardanne, Provence. This internship spanned from May 15 to September 11. Throughout this period, I collaborated with Thibault Langlart, a final-year master's engineering student, as fellow teammates within the scope of the Novabot project. Our activities were conducted at the **ID-Fab** facility, with oversight from our supervisors: research engineer Francois Bernier from the Mines Saint-Étienne Institute and Dr. Julien Serres from the *Institut des Sciences du Mouvement*.

The central objective of the Novabot project is to seamlessly integrate a floating drone named the "ID-FLY airship," tailored for theatrical applications. This drone is intended to offer audiences an alternative perspective of the performance scene. In the context of this project, our specific role was to automate the drone's behavior, enabling it to sustain a predetermined distance from the artist on stage.

Our active participation was centered around the automation phase of the project. To achieve our objectives, we engaged in a range of tasks, including the installation of the ROS framework on the Raspberry Pi card, adapting the Luxonis AI camera for use as a position sensor, constructing an initial dynamic model, and developing the flight control system. Beyond these technical endeavors, we also contributed to the project's artistic demonstration alongside Ph.D. student Yousra Mansar. Yousra's leadership is integral to the artistic research conducted as part of her thesis at Laboratoire d'Etudes en Sciences des Arts (Aix Marseille Université, LESA EA 3274) (LESA) in Aix-en-Provence.

3 State of the Art

3.1 The mini blimps

The last few years have seen particularly rapid technological progress in a number of areas, including aerial drones, or Unmanned Aerial Vehicles (UAVs). Despite this, there are still have not yet been resolved, particularly with regard to their autonomy and the safety of those around them. This is where airships, also known as Lighter Than Air Robot (Lighter Than Air Robot (LTAR)). These drones offer a number of advantages: in particular, the energy to maintain their altitude, since they exploit Archimedes' buoyancy, and their size makes them easy to spot and minimizes the risk of accident. Minimize the risk of an accident. In addition to this, they have the mobility of aerial drones and can therefore easily explore areas considered inaccessible by land.

Airships with a wingspan of less than 2 meters are known as mini-airships. Our project NOVABOT is on the borderline of this category, measuring 2 meters in length. If we look at the work that has been done on these robots, we can see that there are three points that should always be taken into account when designing a mini-blimp. Firstly, a LTAR must have a particularly low mass to be able to float in the air, which places constraints on the equipment it will carry. Secondly, its dynamics are particular because of its shape and inertia. Finally, in the case of autonomous control, not only can the engines be placed in very different places depending on the model, but the airship is also subject to variables such as air pressure, movement, and temperature. The aim of this section is to present various mini airship projects and different solutions for these and other relevant issues.

3.1.1 Similar projects

Firstly, there is the project by Oh et al. [15], a mini-drone with an envelope 2 meters long and weighing 1.2 kilograms. This drone is designed for indoor use and is intended to have images projected onto it. It has six ultrasonic sensors to assess the distance to obstacles, a battery, a microcontroller and six servomotors. These motors can control translation in all three axes, as well as yaw and roll. The robot therefore has 5 degrees of freedom, and its control is a controller Proportional Derivative (PD) for each of these degrees. We therefore have a system with five errors for five independent controls, because two motors together take care of the longitudinal movement. Finally, in order to project images, the mini-blimp is fitted with an infrared marker. It is then tracked by an infrared camera linked to a computer which, based on the state of the airship, deduces in real time the transformation to be applied to the projected image to ensure that it does not appear distorted.

Zufferey et al. have designed a mini airship with an envelope measuring $110 \times 60 \times 60$ cm and three motors: one for altitude, one for longitudinal movement and one for yaw. Its sensors are a camera, an anemometer, an altitude sensor and a piezoelectric gyroscope, all linked to an

3 STATE OF THE ART

8-bit microcontroller with a Bluetooth module and powered by a 1200mAh battery (Fig. 1). It uses visual information to find its way around a room whose walls have specific patterns, thanks to a deep learning neural network. It also has a battery life of 2 to 3 hours, which is quite long for this type of robot.

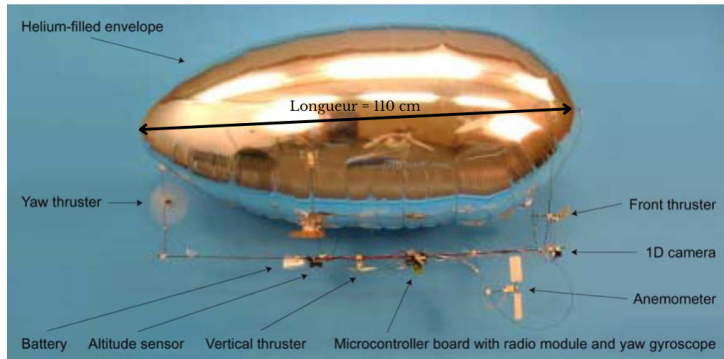


Figure 1: Mini-Blimp, from Zufferey et al. [34].

The mini-blimp developed by Ohata et al.[16] has dimensions quite similar to those of our mini-blimp: it measures $170 \times 60 \times 60$ cm for a mass of 300g including the envelope (178g if not included), but uses only three motors and can therefore only control its longitudinal movement, its altitude and its yaw. What's more, it is remotely controlled via the Internet, as is currently done with NOVABOT. A PD controller has been tested in simulation with satisfactory results, but has not been implemented on the real robot.

Gonzalez's team approached the development of a mini-glider from a different perspective, starting with a commercially available model. The model selected measures 132×94 cm and, like its predecessor, has three motors to control altitude, longitudinal movement and yaw. The team added two ultrasonic sensors to detect obstacles in front of and below the drone, a battery, and a custom electronic board to control the motors and provide communication with a PC. This mini-drone is controlled either by PID or by fuzzy logic, except that the sensor measurements are corrected using a Kalman filter. Fuzzy logic is a method of approaching a problem by defining variables that would normally be considered Boolean, but assigning them a value between 1 and 0. In this case, it is a sequence of if-then to determine the commands to be sent to the motors as a function of the robot's speed and the error in its position relative to a target. Their experiments showed that the PID controller obtained slightly better results but that its parameters were subject to the environment, unlike a fuzzy logic controller, which will therefore be more versatile.

Another mini-blimp was designed by Zhang et al. [32]. This one has an envelope in the shape of an ellipsoid of revolution, but along the z axis, and also communicates with a computer on the ground. It also has five motors: two along the x-axis for longitudinal movement and yaw, two vertical motors for altitude and roll, and one for lateral movement (Fig. 2). It is also

3 STATE OF THE ART

controlled by PID. This robot also has a camera trained to detect and follow a human hand using a neural network. It is capable of recognizing a horizontal or vertical movement of this hand and turning on itself in this case.

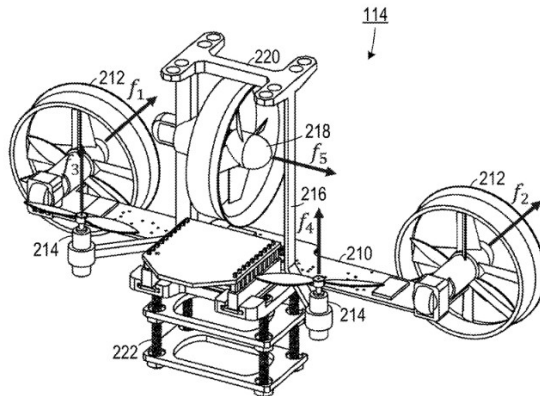


Figure 2: Mini blimp basket from Zhang [32].

Gorjup and Taliokapis [8] also considered the challenge of building the most economical mini-blimp possible. The team first selected an envelope from several available on the market, based on its ability to retain helium and its mechanical properties. Although the 'Bubble' material showed very good results, the balloon in question could only lift 40 grams. It is therefore an envelope made of micro-sheets of Qualatex shaped like a saucer with a diameter of 91cm. For the robot's structure, the basket was 3D printed to accommodate a Raspberry Pi Zero W, a 500mAh Li-Ion battery, three motors (two in the x axis, one in the z axis) and a camera (Fig. 3). However, the team noticed that placing the basket eccentrically to the envelope made the drone more resistant to disturbance (Fig. 4). This mini-blimp is controlled by a "carrot chasing" algorithm presented in [22] and communicates with a computer via ROS. The project is open-source and has its own website, open air ship.

The mini-blimp designed by Gonzalez et al. [7] is also an open-source project and has a git blimp SNN. Its originality lies in its number of motors: it has only two, arranged along the x-axis, but the team has added a servomotor to rotate them along the y-axis, so that it can control altitude (Fig. 5). The drone uses a Raspberry Pi Zero W communicating via ROS. For control, the team tested a simulator and a real robot using a PID controller, an artificial neural network and an impulse neural network. Although all three methods gave satisfactory results, the impulse neural network controller consumes less energy by the motors and is therefore the preferred choice.

Finally, Ikeda et al. propose a quite original mini-blimp [12]. This uses a spherical balloon about 80 cm in diameter as its envelope and is steered by a wind tunnel system, with the aim of making indoor flight as pleasant and safe as possible (Fig. 6). The microblowers used operate at a frequency of 26 kHz for their piezoelectric part, for example, so that they cannot be heard by humans (Fig. 7). The robot also has a Raspberry Pi Zero and a camera, and is powered by a 3S 450 mAh battery. It should be noted that it is hand-controlled, so a control algorithm for

3 STATE OF THE ART



Figure 3: Mini-blimp 3D printing basket [8].

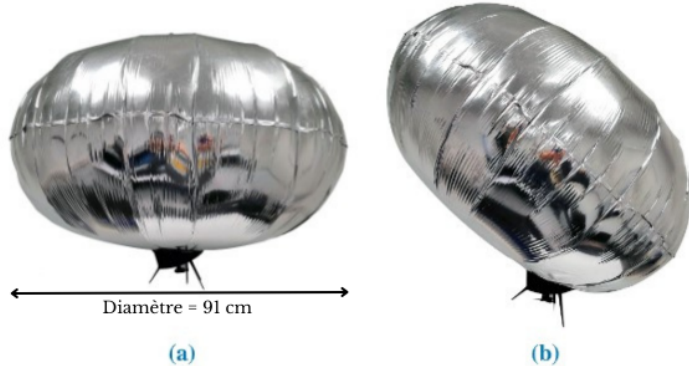


Figure 4: Possible positions for the basket [8]: centered (a) and eccentric (b). In the end, configuration (b) was chosen.

this type of propulsion does not yet exist.

However, the most successful and best-documented project is Georgia Tech's mini-blimp GT-MAB [30, 3, 31, 23, 25, 24, 26, 19, 4, 9]. It is a mini-blimp whose envelope is an ellipsoid of revolution along the z axis, measuring $46 \times 72 \times 72$ cm (Fig. 8). It has four then five motors (two along the x-axis, one along the y-axis and two along the z-axis) and various sensors, including an inertial measurement system (Fig. 9). Again, control is by PID. What's particularly interesting about this robot in our case is that it too is dedicated to interaction with humans. Initially, the mini-blimp had no camera, but it soon received a Red Green Blue Distance (RGBD) [31] in order to detect human faces using the Viola and Jones method [28] and to follow them. GT-MAB blimp was then equipped with a deep neural network to detect human faces and hands and react to certain simple movements [30], as well as an LED panel to indicate recognized gestures

3 STATE OF THE ART

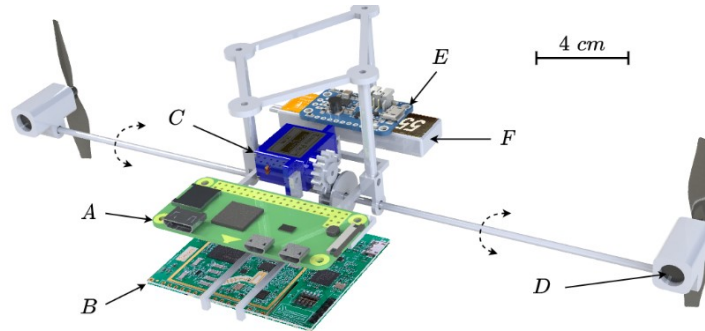


Fig. 2. Scheme of the proposed airship design. (A) Raspberry Pi W Zero; (B) 24 GHz Infineon Radar Position2Go; (C) Sub-micro Servo SG51R; (D) 8520 Coreless Motor; (E) PowerBoost 500 Basic; (F) 550mA 3.8V Li-Po Battery.

Figure 5: Mini blimp basket from Gonzalez et al. [7].

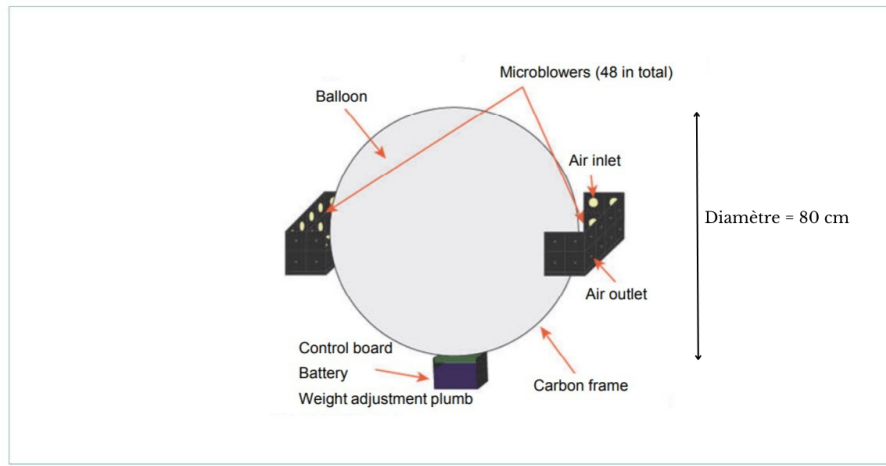


Figure 6: Diagram of airship from Ikeda et al. [12].

to users.

From these different examples, we can draw several common points between mini-blimps. Firstly, their envelope is an ellipsoid of revolution along the x or z axis. They generally have between three and six motors and communicate with a terrestrial computer for the calculations made by the algorithms. Finally, they are generally controlled either by PID or by a neural network.

3.1.2 Related works

Of course, some scientific work may also be very relevant to our situation, without being the development of a mini-blimp. For example, Iida was interested in a visual odometry system applicable to Unmanned Aerial Vehicle (UAV)s [11, 10]. He took his inspiration from bees

3 STATE OF THE ART

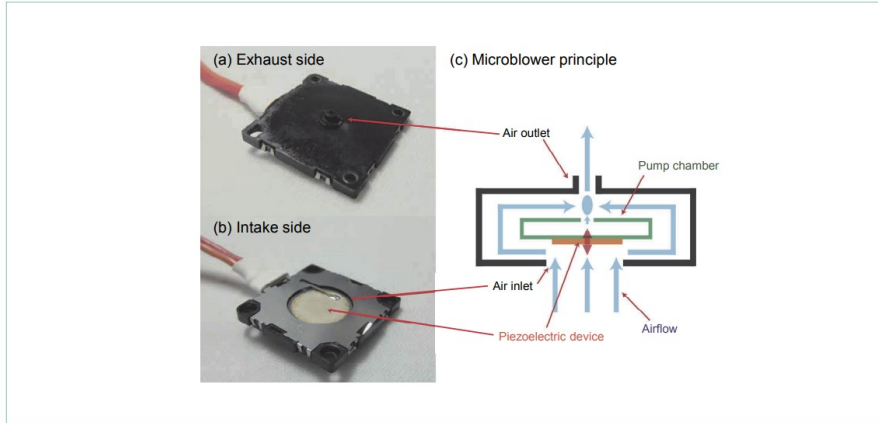


Figure 7: How a micro blower works [12].



Figure 8: First version of GT-MAB by Georgia Tech, USA [23].

in a biomimetic approach, using a Reichardt motion detection model on a panoramic camera mounted on a rail and then on a 2.3-metre-long airship. His experiments showed satisfactory results in an indoor environment, provided that the airship always followed the same route. According to Iida, this system could be particularly effective for landings.

In keeping with his biomimicry approach, Dr. Julien Serres (my tutor) has produced a state-of-the-art report on aerial drones inspired by insects [20]. In addition to airships, the paper discusses hovercrafts, rotary-wing drones and micro-drones. Also explored are bio-inspired sensors for aerial drones and various techniques for guiding UAVs using different bio-inspired visual sensors.

On another subject, Tobita was also interested in airships, but with an idea of augmented reality [27]. He has developed a system that can detect an airship from markers placed on it, and provide a user with additional information such as images projected onto the airship using appropriate glasses. Pressure sensors could be used to take human-robot interaction a step

3 STATE OF THE ART

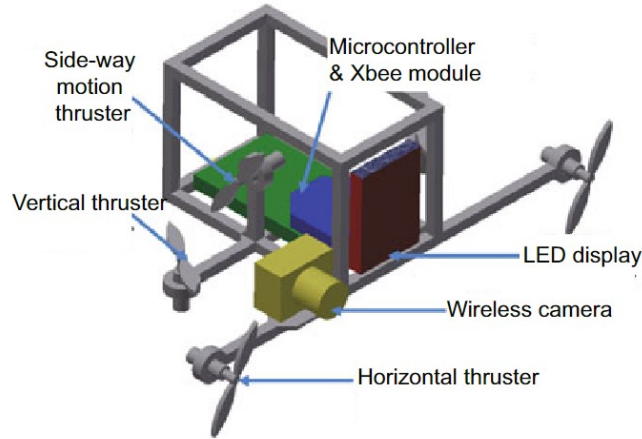


Figure 9: Mini-blimps Basket GT-MAB [30]

further by causing the robot to react when touched by the user.

Finally, Rossouw [18] presents a state of the art of airships, bio-inspired or not, as well as automated control systems. She also presents an airship designed to explore and locate outdoors. It is shaped like a sphere, 53 cm in diameter, and is propelled by five fins (Fig. 10). It can be controlled either manually or using a PID algorithm. This particularly recent work may represent an interesting new alternative for silent and harmless aerial drones.

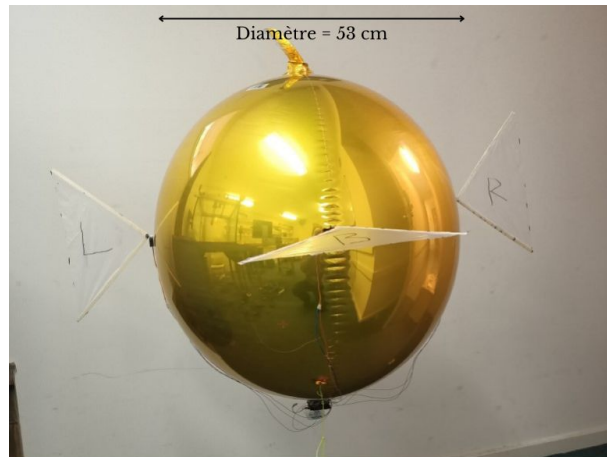


Figure 10: Fin-propelled airship [18]

4 Research groups involved in NOVABOT

The project NOVABOT is developed through the collaboration of these three organizations:

-ISM (Institut des Sciences du Mouvement - Etienne-Jules Marey), Luminy campus, Marseille;

-LESA (Laboratoire d'Étude en Science des Arts), Schuman campus, Aix-en-Provence;

-ID-Fab - EMSE (Innovation, Design-Fabrication - École des Mines de Saint-Étienne), Georges Charpak Provence campus, Gardanne.

4.1 ISM (Institut des Sciences du Mouvement)

The Institut des Sciences du Mouvement Étienne-Jules Marey is a joint research unit under the supervision of Aix Marseille University Aix Marseille Université (AMU) and the National Center of Scientific research (CNRS in French). The latter is attached to the ISM mainly through the institute of biological sciences (INSB), which is the main home institute. Together with other three secondary institutes: l’Institut des Sciences de l’Ingénierie et des Systèmes (INSIS); l’Institut des Sciences Informatiques et de leurs Interactions (INS2I), et l’Institut des Sciences Humaines et Sociales (INSHS).

This institution concentrates in the research of movement, seizing the study of every possible angle. A wide variety of sciences are practiced here, including neuroscience, robotics, physiology, biomechanics, but also psychology and sociology. Interdisciplinary is one of the institute’s key aspects, and the different approaches are brought together in order to obtain a global vision that is as complete as possible of the production of movement. The organization chart in figure 11 shows the re-structuration that started the 1st January 2023.

Its researchers are divided into three teams, each focusing on two areas. There is the Biomechanics Bioengineering team - BMI - (Biomechanology and Integrative Biomechanics axes), the Behavioural Dynamics and Cognition team - DynamiCC - (Sensorimotor, Perceptual and Psychological Processes and Context, Adaptation, Intervention axes), and the Sensorimotor, Perceptual and Psychological Processes and Context, Adaptation and Intervention), and finally the Bio-Inspired Systems team - SBI - (Biorobotics and Bio-Inspired Mechanics axes).

Thanks to the multidisciplinary nature of its activities, ISM works with a number of different business clusters. Its research is supported by numerous long-term corporate partnerships, such as: AG2R, Safran, Thales, Nike and Stellantis, as well as other national agencies such as "Agence Innovation Défense (AID)" which reports to the French Direction Générale de l’Armement (DGA), etc. Funding for ISM’s research work is partly provided by the Centre National de la Recherche Scientifique (CNRS), although the laboratory’s annual endowment is relatively stable over the past decade, from 220,000 euros in 2011 to 190,000 euros in 2023.

4 RESEARCH GROUPS INVOLVED IN NOVABOT

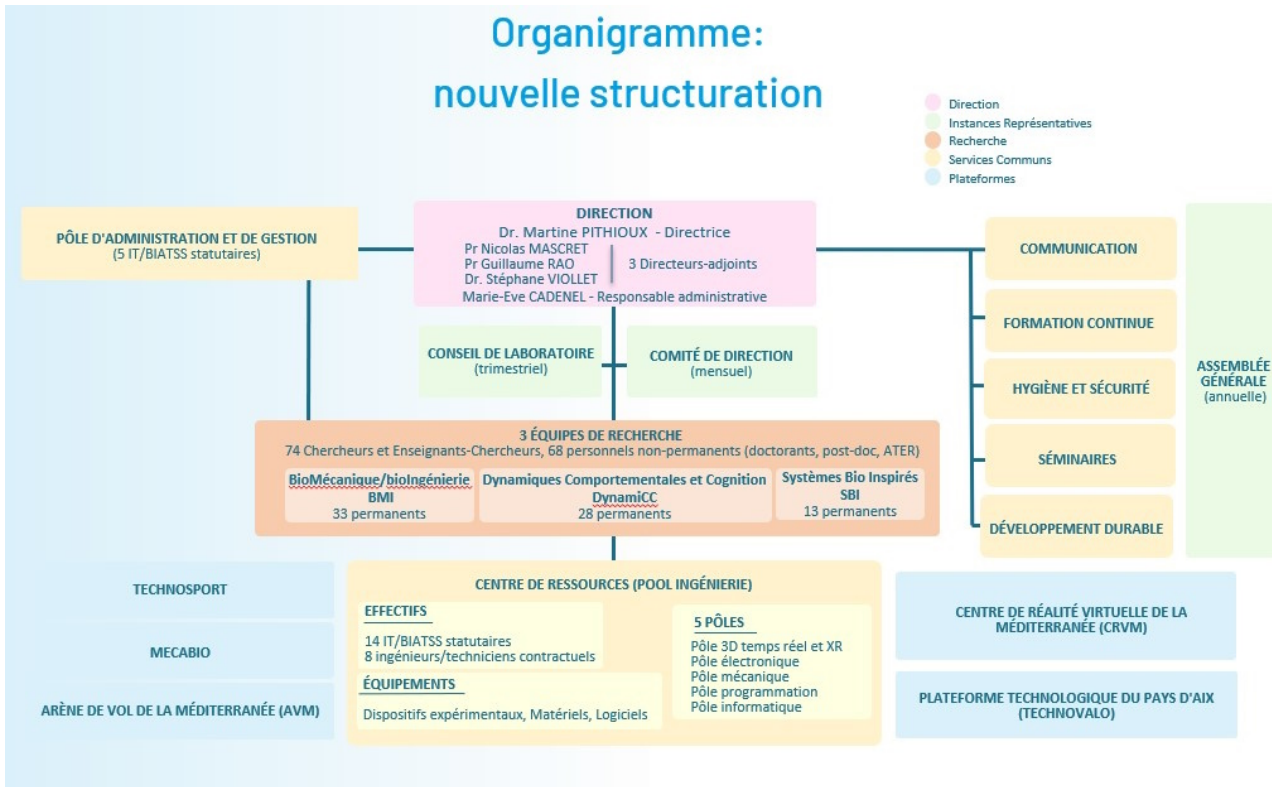


Figure 11: Organisation chart of the Institut des Sciences du Mouvement - Etienne-Jules Marey (CNRS/Aix Marseille Université, ISM UMR7287).

Source : <https://ism.univ-amu.fr/fr/l'institut/organigramme>.

ISM relies on external funding. Given the multidisciplinary nature of the work, the partners behind this funding are varied in nature.

It also has a recurrent operating budget granted by its scientific sponsors (AMU 50% and CNRS 50%) of approximately €380,000 per year for a total staff of 170, including both permanent and non-permanent staff. This sum represents only a tiny fraction of the funding used by ISM, since the ISM, as research, is now financed by research contracts, which represent several million euros each year.

ISM is equipped with 5 cutting-edge technology platforms focused in working with measurements of behaviors, working with all types of participants from high-level sportsmen and women to the elderly. From high-level athletes to the elderly and disabled. Which are the following:

- **TechnoSport Marseille Luminy** combines top-level sport with scientific research;
- **The Mediterranean Flying Arena Platform** built for research in biorobotics;

- **Center For Virtual Reality Of The Mediterranean** focused on the study of human movement;
- **Aix-en-Provence Technology Platform** which promotes innovation and technology transfer in the field of (bio)mechanics;
- **Plateform Mécabio** to perform mechanical tests on all types of materials, biomaterials, or biological matter.

4.2 LESA (Laboratoire d'Etude en Science des Arts)

The Laboratoire d'Études en Sciences des Arts (LESA), research unit number 3274, is an entity bringing together the various artistic sectors of Aix-Marseille University. It is affiliated with the UFR ALLSH (Unité de Formation et de Recherche Arts, Lettres, Langues, Sciences Humaines et Sociales) and is part of the doctoral school ED 354 Langues, Lettres et Arts. LESA supports research and specialized work in the disciplines taught by its teacher-researchers, covering the following areas:

- Visual and performing arts
- Cinema
- Aesthetics and arts sciences
- Cultural mediation
- Music and music sciences

4.3 ID-Fab - École des Mines de Saint-Étienne

ID-Fab (Innovation, Design-Fabrication) is a specialized technology platform that brings together the skills of Mines Saint-Étienne on the George Charpak Provence campus, focusing on connected objects and sensory interfaces. The aim of ID-Fab is to strengthen the dynamic between research, training, and support for companies in their projects, by encouraging the pooling of skills. The referents of this platform are:

- Sylvain BLAYAC: Project Manager
- Roger DELATTRE: Platform Group Manager
- François BERNIER: Space R&D / Prototype Manager
- Pierre-Laurent CODDET: Research Manager
- Acacio MARQUES: Teacher-Engineer

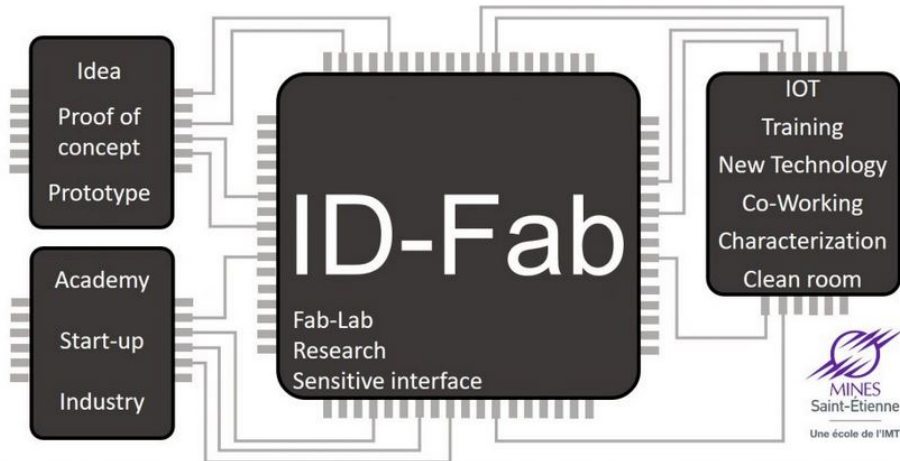


Figure 12: ID-Fab functioning.

Source: <https://www.mines-stetienne.fr/recherche/plateformes/id-fab/>.

During this internship, I was mainly in contact with François Bernier and Julien Serres, with whom we discussed the progress of the airship robotization project. My internship mainly took place on the George Charpak campus in Gardanne, where the ID-Fab technology platform is located.

This platform trains students, interns, and PhD students all year round, but also and above all supports more and more companies in their prototyping development, notably thanks to their varied 3D printing equipment.

Indeed, we've noticed a boom in the platform's support for small and large companies alike. Indeed, during my internship, the platform succeeded in establishing contacts with numerous companies who used their services to bring projects to accomplishment or to create prototypes of varying complexity.

5 State of the art in mini airships

The aim of this section is to present the ID-Fly mini-blimp and describe its state at the start of the project.

This prototype didn't face huge changes, because, although progress was made during this period, there wasn't enough time to be tested on the airship. Besides the time, the airship is very fragile, and essential to the presentations of NOVABOT project throughout Youssra Mansar's PhD thesis. Therefore, we decided to not make drastic changes on its design or code that would compromise the integrity of the prototype, so it can work in the coming presentations.

Nevertheless, ID-Fab will be able to make a better quality clone next year, as we already point the deficiencies in the current prototype.

5.1 Functions of ID-Fly airship

The ID-Fly airship's role is to give the spectator a different point of view of the scene, to accomplish this the airship has to maintain the correct distance and angle with the artist's face and stream the video of the artist's face.

The Luxonis camera takes the image of the artist, from the image it calculates the position and shares the video backstage, then the backstage will stream the video on the big screen. If the drone is flying autonomously then the control system will pilot the drone to correct the position, otherwise, the Raspberry Pi provides a user interface that allows the backstage to pilot the drone. The user interface is described in the figure 13.

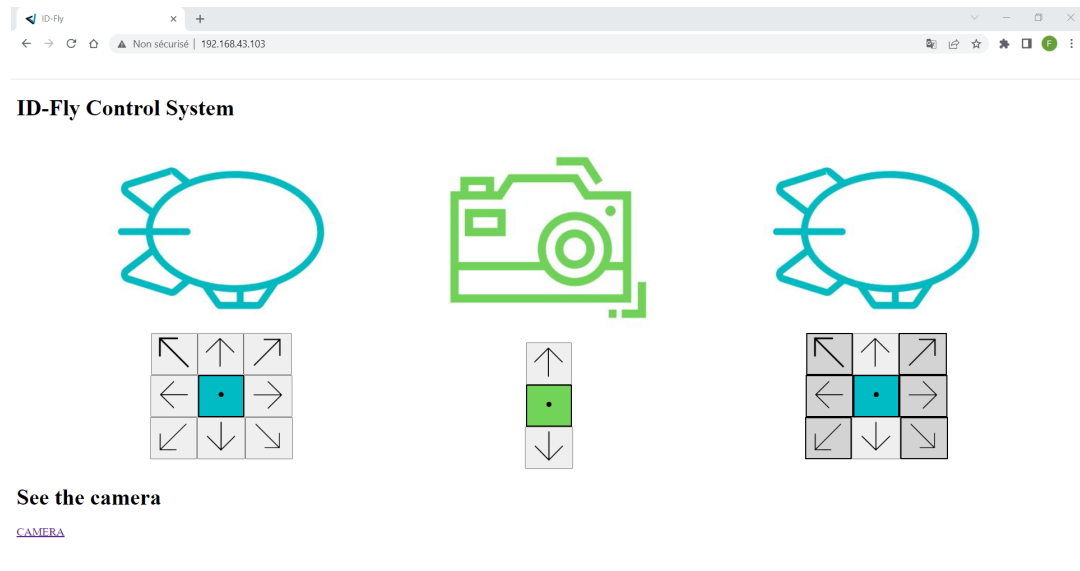


Figure 13: User Interface for backstage.

When we joined the project the user the blimp was able to fly controlled by the computer as we can see in the figure 13, the blimp was sending correctly the images to the computer to stream to the big screen.

5.2 Envelope and structure

Most of the airship's volume is taken up by its envelope. This is made of polypropylene with a thickness of 180µm. It is an ellipsoid of revolution along the x-axis, with diameters of 2 meters and 0.75 meters respectively (Fig. 14). It has three ailerons at the rear. The envelope is filled with helium and has a capacity of 600 liters.

5 STATE OF THE ART IN MINI AIRSHIPS

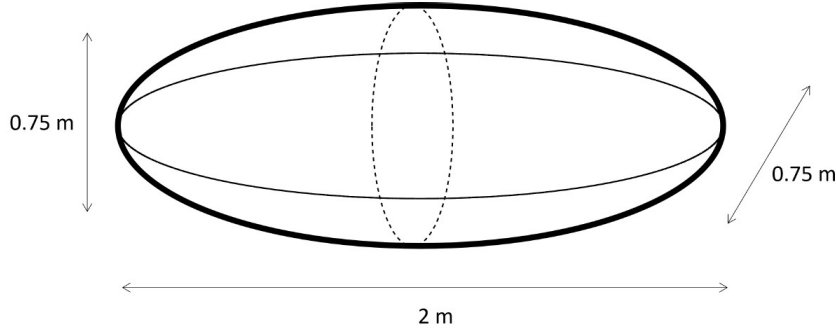


Figure 14: Envelope of the ID-Fly blimp.

When we received the prototype, one of the first things that needed a change was the envelope. After many internships, the state of the envelope is fragile and has already been repaired several times, which affects its performance (helium leaks). Therefore, we tried to contact the manufacturer in the USA but he no longer responds. We had to find another manufacturer in Europe to remedy this problem. The German company Windreiter UG met our requirements perfectly, they have an envelope of the same shape, measuring 2.06 meters by 0.82 meters and with a volume of 737 liters. This envelope will be made of Tritax silver.

The envelope has four attachments, one for each rod, to connect it to the main rod running along the x-axis and supporting the other parts of the structure (Fig. 15). At present, the connections are made by simple cables placed along the rod and held in place by pieces of unheated heat-shrink tubing. In addition to these cables, the components on the rod are a Raspberry Pi board and camera, four motors and a gondola. Each of these elements has a support to hold it in place, which were made by 3D printing in resin 4000 cured by ultraviolet rays using aForm 3+ de Formlabs. However, these components have been designed to be as light as possible, sometimes to the detriment of strength. As a result, parts can often break, even if care is taken when handling the airship. What's more, the parts sometimes slip. This problem should be solved by adding a hole to the parts and the main rod to allow a pin to be added.

The mini airship is motorized by four DC motors (Ref. Yiqigou 4Pcs RC Quadcopter A-B Motor Positive and Negative 720 Drone Motor Accessories Suitable for Syma X5 / X5C / M68). The first propulsion unit enhances its thrust by employing a gear mechanism that drives a large helical propeller. Positioned at the center of the rod, this mechanism exerts force along the z-axis, allowing for precise altitude control. Similarly, the second propulsion unit utilizes the same mechanism as the first, but it is strategically placed at the rear of the airship. This placement enables thrust along the x-axis, thereby enabling effective control over longitudinal movement.

The remaining two propulsion units, located at the rod's ends, are responsible for managing

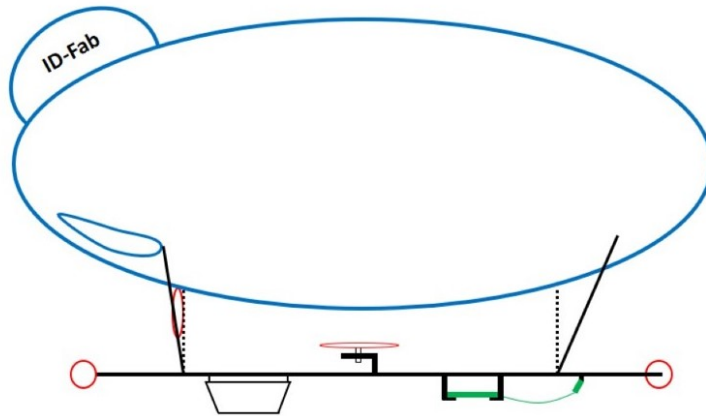


Figure 15: Diagram of the mini-blimp ID-Fly.

the robot's heading. These thrusters lack a propulsion force enhancement mechanism, resulting in comparatively lower thrust output. Notably, their propellers are custom-designed using 3D printing technology. The first two engines are equipped with four-bladed propellers set at a pitch angle of 15° , whereas the two lateral thrusters feature three-bladed propellers with adjustable pitch angles to optimize performance.

Additionally, the airship features a basket that serves the purpose of carrying batteries and any necessary weights for adjusting the airship's buoyancy 16.

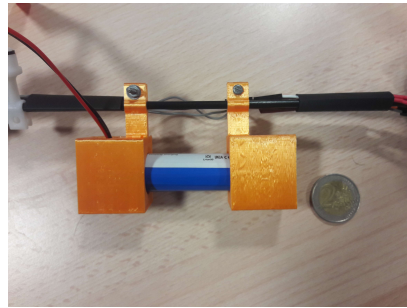


Figure 16: New battery with mounting parts.

5.3 Mass balance and forces exerted

To ensure the airship's functionality, it's imperative that it possesses the ability to achieve buoyancy, effectively counteracting its own weight through the principle of Archimedes' thrust (Fig. 17). In pursuit of this objective, our approach involves determining its maximum load-bearing capacity. This involves considering a scaled-down version, resembling a mini-blimp,

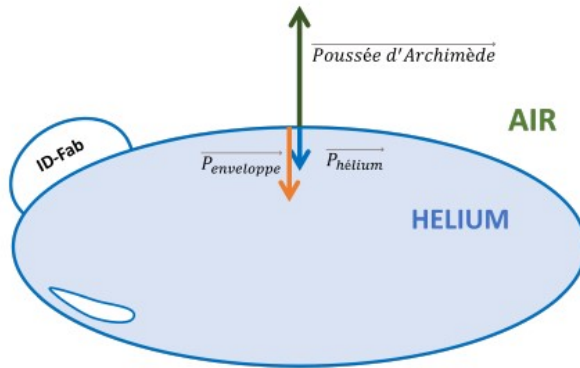


Figure 17: Balance of forces applied to the steering system.

composed of a 600 L envelope primarily filled with helium, alongside the remaining structural components.

In this scenario, the airship is subjected to two fundamental forces: its inherent weight and the force attributed to Archimedes' principle. The respective densities of helium and air under standard atmospheric conditions (20°C and 1 atm), as well as the mass of the envelope, are provided as follows:

$$\begin{aligned}\rho_{helium} &= 0.178 \text{ kg/m}^3 \\ m_{enveloppe} &= 0.300 \text{ kg} \\ g &= 9.81 \text{ N/kg} \\ V &= 600 \text{ L}\end{aligned}$$

Indeed, the densities of the gases involved will be influenced by the temperature of the experimental site as well as its altitude. This variability is the reason behind our utilization of weights, which allow us to effectively nullify the buoyant effect of the mini-blimp prior to each performance or experiment.

By applying the fundamental principles of dynamics along the vertical z-axis, we derive the following equation:

$$a_z \cdot m_{blimp} = -g \cdot m_{blimp} + g \cdot m_{DisplacedAir} \quad (1)$$

Our objective is to establish an airship mass that maintains equilibrium, resulting in zero acceleration or buoyancy. Consequently, we can set $a_z = 0$, leading to the following equation:

$$m_{dirigeable} + m_{DisplacedAir} = 0 \quad (2)$$

It becomes into:

$$m_{enveloppe} + m_{helium} + m_{useful} - m_{DisplacedAir} = 0 \quad (3)$$

Considering m_{useful} as the mass of the airship, encompassing the structure and onboard electronics, excluding the envelope and helium, we arrive at the following expression:

$$m_{useful} = V \cdot \rho_{DisplacedAir} - m_{enveloppe} - V \cdot \rho_{helium} \quad (4)$$

To then obtain:

$$m_{useful} = 0.320 \text{ kg} \quad (5)$$

To ensure caution, considering the approximations involved in measuring the envelope's mass, we will adopt a mass of m_{useful} (= 300 grams) for subsequent calculations.

From this, we can deduce that the envelope filled with helium can effectively lift a maximum mass of 300 g. Proceeding further, we proceed with the calculation of the airship's useful mass:

Matériel	nacelle (moteurs compris)	panier	batterie	Raspberry + driver	autres struc- tures	Total
Poids (grammes)	110	35	40	41	20	246

Figure 18: Balance of the airship's useful mass. From [21].

While the initial configuration of the airship was suitable for flights with manual control, it proved inadequate for our specific objectives upon receipt. The structure exhibited an unintended pitch angle inclination (Fig. 21), resulting in an undesired torque during flight. This torque caused the airship to veer off course during each flight. In response, we undertook a reconfiguration of the weight distribution to achieve the desired level of stability. Furthermore, our efforts focused on ensuring the accurate implementation of force dynamics throughout the entirety of the flight, allowing us to achieve the desired control and maneuverability.

5.4 Embedded Electronics

The mini-blimp has an on-board computer in the presence of a Raspberry Pi Zero W weighing in at 9 grams, with Debian 10 installed as the operating system on a 128 GB micro-SD card. The card is powered by a single-cell 1800mAh 3.7V battery, enough for around 20 minutes' use.(Fig. 19). However, as the Raspberry Pi Zero W consumes 2A at 5V, a Lipo SHIM system is used to boost the supply voltage. In addition, the Zero W is not designed to drive four motors at the same time, which must be done to control the airship. A motor shield has therefore been added with two L298P drivers, each capable of controlling two motors, with a four-quadrant chopper to enable control in both directions.

Finally, the board is also connected via a CSI connector to a Raspberry Pi camera, weighing

6 PROGRESS MADE IN THE INTERNSHIP

just 3 grams, with a python program to send the image to a web page in real time. This page is on a web server created when the Raspberry Pi is started up, and can also be used to control the airship using a joystick.

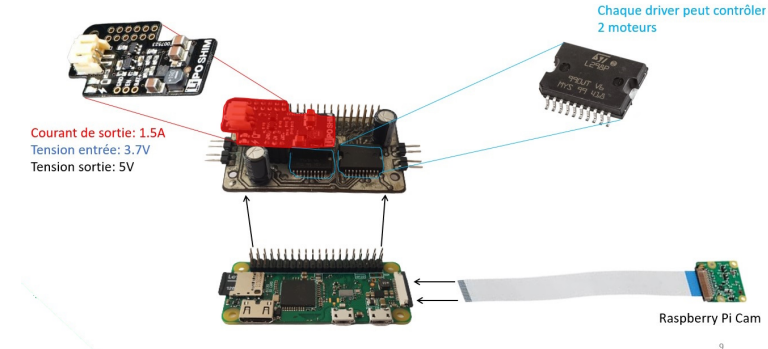


Figure 19: Raspberry Pi Zero W with a converter, shield, drivers, and camera. From [21].

6 Progress made in the internship

6.1 Camera

The primary objective of this internship centered around automating the drone's behavior, enabling it to track the subject while maintaining a consistent distance. To accomplish this goal, we employed the Luxonis OAK-D-IoT-40 camera. This camera system comprises a color camera and two pairs of stereo black and white cameras. Notably, it is augmented with artificial intelligence capabilities rooted in deep learning techniques.

Leveraging its deep learning capabilities, the camera is equipped to recognize human faces and extract pertinent information such as their precise location, distance from the lens, and even the direction of their gaze. The two sets of stereo cameras facilitate three-dimensional vision of the surroundings. Furthermore, the camera integrates a third lens dedicated to capturing color information, thus generating a 3D color RGBD image.

The integration of the camera posed several challenges. The foremost concern was the camera's weight, which stood at approximately 39 grams. This was a critical constraint, given that the current mini blimp was limited to carrying a payload of 300 grams.

In our endeavors to alleviate the weight, we explored the possibility of eliminating the radiator, which accounted for 15 grams of the camera's weight. However, despite our efforts, we were unable to locate an alternative cooling solution that weighed less than 15 grams. In our assessment of the radiator's necessity, we conducted temperature rise measurements using an ETS320 thermal imaging camera. This specialized camera, designed for test benches and research purposes, was employed in a room set to a temperature akin to that of a theater stage (20°C). Over a span of 20 minutes—the duration of a performance—the temperature escalated

from 32 to 65 degrees Celsius. This experiment led us to conclude that the radiator was indeed indispensable.

In addition to the camera's weight, we were also obliged to factor in the weight of the micro USB-C cable, responsible for transmitting data to the Raspberry Pi. This cable weighed 34 grams. To mitigate this weight, we opted to strip the cable of its sheath and shorten its length.



Figure 20: Caméra Luxonis OAK-D-IoT-40. Size: 60mm large, height 45mm, large 25mm; mass: 45g in technical documentation.

The second challenge revolved around the power supply for the Luxonis camera. In previous iterations, we utilized a Raspberry Pi Cam v2, which drew power from the Raspberry Pi itself. However, due to the distinct dimensions and increased functionalities of the Luxonis camera, its power consumption was considerably higher. My measurements indicated a consumption of 0.9 A at 5 V. Consequently, we can extrapolate the energy requirement for a 20-minute performance (equivalent to $\frac{1}{3}$ of an hour):

$$E_{Luxonis} = 0.9 \times 5 \times \frac{1}{3} = 1,5 \text{ Wh} \quad (6)$$

Knowing that current battery Lithium-Polymer (Li-Po) is a 1S 1800mAh 3.7V, to maintain the same voltage, we know that our new batteries' capacity should be:

$$\frac{1,5 + 1,8 \times 3,7}{3,7} \approx 2,205 \text{ Ah} \quad (7)$$

After searching through various models, we chose the new battery with a capacity of 2.6 Ah, and a mass between 36 and 48 grams. To place this new battery, I designed a new battery support (Fig. 16).

6.2 Dynamic modeling of ID-Fly airship

The ID-Fly's dynamic model was designed to fly as an indoor airship with low speed which, in these conditions, most perturbations can be neglected. As a result, we decided to control the motion of the drone with three degrees of freedom (DOFs). The thrusters of the blimp are designed to move in the vertical plane (Z-axis), and the horizontal plane (X-axis) and rotate around the vertical axis (Yaw-axis ψ). In the following paragraphs, we will describe the forces and the equations used to build the dynamics of ID-Fly airship, the reference frame was located in the center of the envelope. We set the following terms where the 3D movement with "X, Y, Z" coordinates describing the position of the blimp. The following angles describe the inclination through the 6 DOFs: $\omega = [\phi \text{ roll}, \theta \text{ pitch}, \psi \text{ yaw}]$,

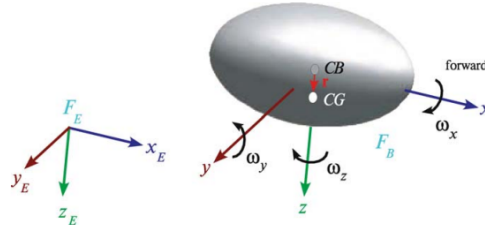


Figure 21: Blimp axis and angles.

To describe the forces applied in the system, we will use the following matrix equations in formulas 1 and 2:

$$m \cdot a = F_R + F_P + F_D + F_C = \begin{pmatrix} F_{R_x} + F_{P_x} + F_{D_x} + F_{C_x} \\ F_{R_y} + F_{P_y} + F_{D_y} + F_{C_y} \\ F_{R_z} + F_{P_z} + F_{D_z} + F_{C_z} \end{pmatrix} \quad (8)$$

$$I \cdot \ddot{\Omega} = M_R + M_P + M_D + M_C = \begin{pmatrix} M_{R_\phi} + M_{P_\phi} + M_{D_\phi} + M_{C_\phi} \\ M_{R_\theta} + M_{P_\theta} + M_{D_\theta} + M_{C_\theta} \\ M_{R_\psi} + M_{P_\psi} + M_{D_\psi} + M_{C_\psi} \end{pmatrix} \quad (9)$$

In formula 1, we describe the linear movement with the output forces $m \cdot a$ giving the direction. In formula 1 the forces involved are: F_R (the restoring forces, including gravity, and helium buoyancy), F_P (Propelling forces, including all thrusters), F_D (Damping forces due to air friction) and F_C (Coriolis and centripetal effects).

In formula 2, we describe the rotation and torque in the system where $I \cdot \Omega$ is the rotational output, and M is the inertial matrix containing rigid body inertia and added mass terms. As we observe the blimp in the second figure, we can start noticing the forces involved in the free-body diagram.

In the second figure (Fig. 22b), we set $P_{X,Y,Z}$ as the thrusters, L is the distance between the two thrusters at gives the turn round axis Z (P_{Y_1} and P_{Y_2}). CV is the center of volume of the Blimp, CM is the center of mass of the drone, d_{VM} is the distance between CV and CM , and d_{MT} is the distance between the center of mass and the bottom of drone. These distances were

6 PROGRESS MADE IN THE INTERNSHIP

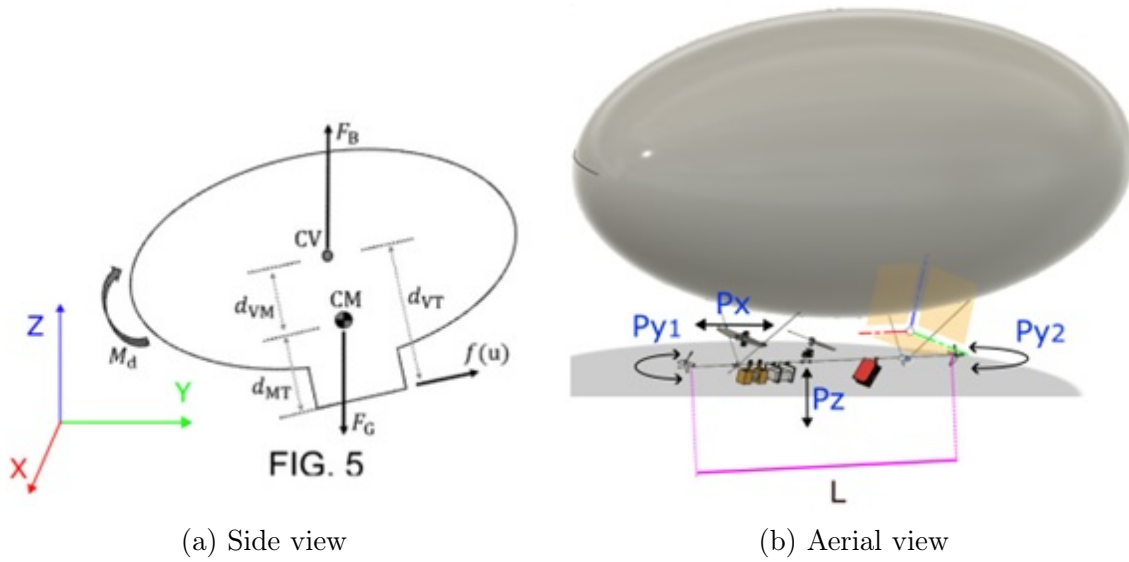


Figure 22: Free body diagram of the ID-Fly blimp.

taken to calculate the torque generated by the buoyancy. When we replace these equations with the current variables, we start noticing that some values are equal to 0, in the Z axis the Coriolis force is 0 because there shall be no rotation in while the blimp is descending or ascending:

$$\begin{aligned} m \cdot a_x &= \left(0 + P_x - D_{VX} \cdot v_x + m \cdot v_y \cdot \psi \right) \\ m \cdot a_y &= \left(0 + 0 - D_{VX} \cdot v_x - m \cdot v_x \cdot \psi \right) \\ m \cdot a_z &= \left((-F_c + F_B) + P_z + D_{Vz} \cdot v_z + 0 \right) \end{aligned} \quad (10)$$

For the second formula:

$$\begin{aligned} I \cdot \ddot{\phi} &= \left(0 + F_B d_{VM} \sin(\phi) - D_{\omega_x} \dot{\phi} \right) \\ I \cdot \ddot{\theta} &= \left(-F_B d_{VM} \sin(\theta) + d_{MT} \cdot P_z - D_{\omega_y} \dot{\theta} \right) \\ I \cdot \ddot{\psi} &= \left(0 + \frac{L}{2} \cdot (P_y 1 + P_y 2) - D_{\theta_z} \cdot \dot{\psi} + 0 \right) \end{aligned} \quad (11)$$

If we add the two matrix equations into one, we could make a simulation matrix that would give us the direction of the drone in 6 DOFs. Even though this matrix would give us a good result for a simulation, the drone will be reduced to 3 DOFs, which are the most relevant movements to be aligned with the face of the actor, this will reduce the matrix to 3 equations that will be used in to calibrate the PID to control the drone's flight.

$$\begin{aligned} m \cdot a_x &= \left(P_x - D_{VX} \cdot v_x + m \cdot v_y \cdot \psi \right) \\ m \cdot a_y &= \left(-D_{VX} \cdot v_x - m \cdot v_x \cdot \psi \right) \\ I \cdot \ddot{\psi} &= \left(0 + \frac{L}{2} \cdot (P_y 1 + P_y 2) - D_{\theta_z} \cdot \dot{\psi} + 0 \right) \end{aligned} \quad (12)$$

6 PROGRESS MADE IN THE INTERNSHIP

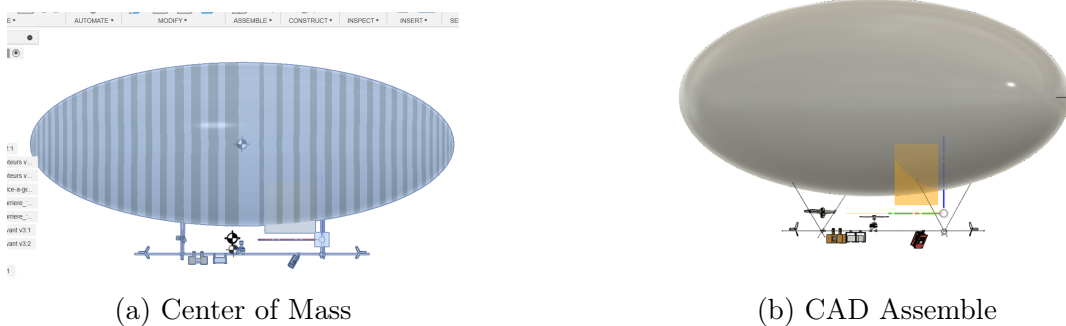


Figure 23: CAD Model

While developing the numerical model, a concurrent virtual model was constructed in *Fusion 360*. This parallel approach was adopted due to the fragility of the model's components. The intricate nature of these components made disassembly a risky proposition, as it could lead to breakage during adjustments.

Utilizing the capabilities of *Fusion 360*, we harnessed its automated functionalities to compute inertia matrices and determine the center of gravity for both individual parts and the entire assembly. This expedited the evaluation process, ensuring precise characterization of the system's dynamics.

$$I = \begin{pmatrix} 6,15 \times 10^{11} & 0 & 0 \\ 0 & 1,77 \times 10^{11} & 0 \\ 0 & 0 & 1,36 \times 10^{11} \end{pmatrix} \quad (13)$$

Furthermore, beyond obtaining parameters for the numerical model, we generated detailed plans for each individual component. These plans were designed to facilitate any necessary modifications in subsequent stages of the project, enhancing adaptability and efficiency.

To ascertain the thrust of the motors and the coefficients of friction, we conducted filming sessions of the robot in flight. Each session involved the robot performing either a straightforward translation or rotation movement. Subsequently, we employed **Kinovea** software to track specific points on the robot and derive the airship's velocity (refer to Fig. 24). However, it is important to note that the airship encountered balance issues during these flight trials, compounded by the fact that we intend to modify the envelope. As a result, there might be uncertainties about the applicability of the collected data. To address this, we are currently conducting additional flight tests, considering the adjustments made to the airship's envelope.

Unfortunately, due to time constraints, we were unable to incorporate the latest flight test data into the current analysis. Nevertheless, this data will be meticulously recorded for the benefit of future interns working on the project.



Figure 24: Kinovea Simulation

6.3 Autonomous system

6.3.1 Goals for the autonomous System

With this project, we are in the situation of a robot evolving in an unknown indoor environment that is likely to change according to the mission. Traditionally, the aim of the robot would be to find its way around this environment by constructing a map, for example using a Simultaneous Localisation And Mapping (SLAM) method. However, our aim here is not to explore the environment, but to place itself at a certain position in relation to an actor that can be likened to a marker, since it is supposed to be easily recognized. What's more, the airship is supposed to be placed by a human hand in front of the actor, so that it already detects him when its autonomous phase begins. Our mission doesn't include any exploration, so there's no need to try to imagine the environment. We can simply place ourselves in the robot's inertial reference frame and move our target there, which will be the actor's head.

6.3.2 Measurement of thrusters

In order to build our numerical model, we had to measure the range forces we could get from each thruster, then measure the output force in our model. In order to achieve this, we designed a support to hold the thruster pointing to the center of the scale. The scale used came from a collaboration with Valentin Divay's PhD thesis, and ex-member of the ID-Fly project. He designed a scale adapted to give a direct measure of the forces, with the right range of sensibility for our project.

In the first measurement, when we were increasing 0.01 volt gradually until we reached 2V with a constant current of 3A. The same test was done pulling and pushing. The following chart will show the two types of thrusters, we have.

6 PROGRESS MADE IN THE INTERNSHIP

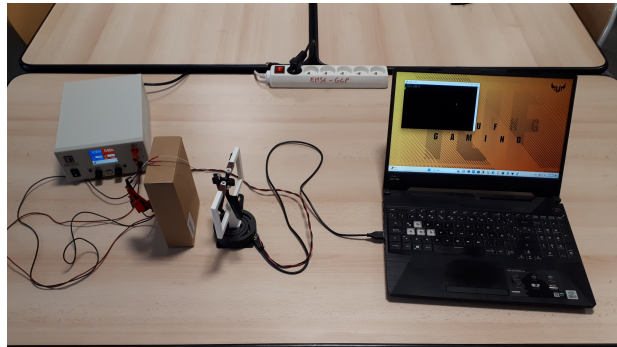


Figure 25: Thrusters measurement test bench.

This step was a challenge as there was no datasheet available, therefore we didn't know the range of power that the thruster could handle. This problem represented an issue as Valentin Divay's needed a broad range for or how fast they would heat up. As a result, 2 thrusters were burned and 1 support was melted (Fig. 26).

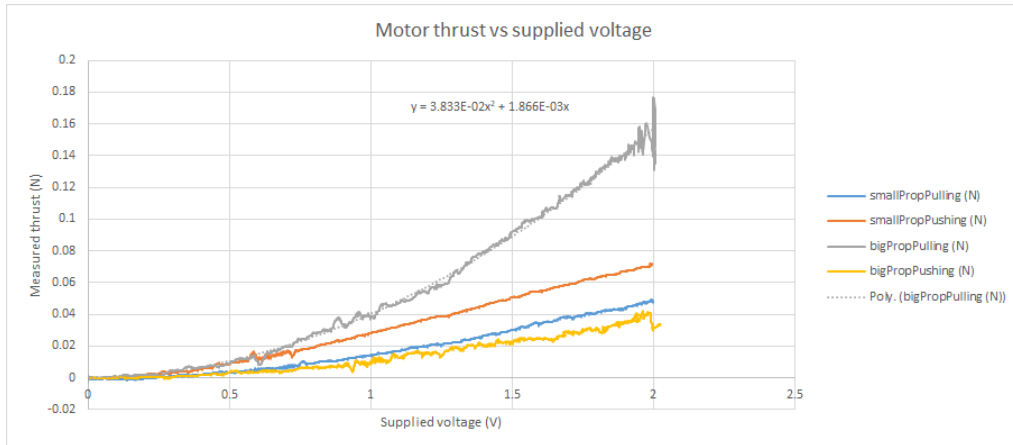


Figure 26: Thrusters gain.

6.3.3 Control algorithm

To automate robot control, we use a PID controller. As seen after modelling the dynamics, we end up with a system with four degrees of freedom for four controls, one for each motor. controls, one for each motor. We place ourselves in the robot frame of reference in the target frame of reference. target reference frame. The state chosen is :

$$\begin{bmatrix} \dot{x} \\ \dot{y} \\ \dot{z} \\ \psi \end{bmatrix} \quad (14)$$

We can then write the equation for the evolution of the system :

$$\dot{X} = \begin{bmatrix} K_{long} \cdot u_{long} - \frac{D_{v_x}}{m} \cdot \dot{x} - \dot{y} \cdot \dot{\psi} \\ K_{latav} \cdot u_{latav} - K_{latar} \cdot u_{latar} - \frac{D_{v_y}}{m} \cdot \dot{y} + \dot{x} \cdot \dot{\psi} \\ K_{alt} \cdot u_{alt} - \frac{D_{v_z}}{m} \cdot \dot{Z} \\ \frac{L \cdot m}{2I_z} \cdot (K_{latav} \cdot u_{latav} + K_{latar} \cdot u_{latar}) + \frac{D_{w_z}}{I_z} \cdot \dot{\psi} \end{bmatrix} \quad (15)$$

With:

u_{long} , u_{latav} , u_{latar} , u_{alt} commands sent to the longitudinal, lateral front, lateral rear and vertical motors respectively

K_{long} , K_{latav} , K_{latar} , K_{alt} constant coefficients specific to each engine such that:
 $m \cdot K_i \cdot u_i = P_i$

From this we got:

$$\dot{X} = \begin{bmatrix} K_{long} & 0 & 0 & 0 \\ 0 & K_{latav} & -K_{latar} & 0 \\ 0 & 0 & 0 & K_{alt} \\ 0 & \frac{L \cdot m}{2I_z} \cdot K_{latav} & \frac{L \cdot m}{2I_z} \cdot K_{latar} & 0 \end{bmatrix} \cdot \begin{bmatrix} u_{long} \\ u_{latav} \\ u_{latar} \\ u_{vert} \end{bmatrix} + \begin{bmatrix} -\frac{D_{v_x}}{m} \cdot \dot{x} - \dot{y} \cdot \dot{\psi} \\ -\frac{D_{v_y}}{m} \cdot \dot{y} + \dot{x} \cdot \dot{\psi} \\ -\frac{D_{v_z}}{m} \cdot \dot{Z} \\ \frac{D_{w_z}}{I_z} \cdot \dot{\psi} \end{bmatrix} = A \cdot U + B \quad (16)$$

Next, we need to define the position of our robot. Looking at the information given by the camera: the position of the target in the image is given as (y_c, x_c) , and its distance in meters from the camera, given as d_c . Note that the position is in pixels and that the image is presented as a NumPy array, so y_c corresponds to the row number and x_c to the column number. Next, we know the resolution and aperture of the camera, so we can deduce the angular error:

$$\begin{bmatrix} err_{\theta_h} \\ err_{\theta_v} \end{bmatrix} = \begin{bmatrix} (x_p - \frac{Res_x}{2}) \cdot HFOV \\ (y_p - \frac{Res_y}{2}) \cdot VFOV \end{bmatrix} \quad (17)$$

With:

Res_x , Res_y the camera's horizontal and vertical resolution

$HFOV$, $VFOV$ the horizontal and vertical openings of the camera

By making a few projections, we obtain the distance from the target to the camera:

$$\begin{bmatrix} d_{cx} \\ d_{cy} \\ d_{cz} \end{bmatrix} = \begin{bmatrix} d_c \cdot \cos(\text{err}_{\theta_v}) \cdot \cos(\text{err}_{\theta_h}) \\ -d_c \cdot \cos(\text{err}_{\theta_v}) \cdot \sin(\text{err}_{\theta_h}) \\ -d_c \cdot \sin(\text{err}_{\theta_v}) \cdot \cos(\text{err}_{\theta_h}) \end{bmatrix} \quad (18)$$

To deduce our position, remember that the camera is positioned in front of the airship by a distance noted d_{cam} and tilted by an angle noted α . We also assume that our reference frame has our target as its origin, but that its orientation is linked to the robot and that the yaw ψ is therefore constantly zero. This allows to define our ψ to be reached as $-\text{err}_{\theta_h}$. Our position noted X_{int} is therefore :

$$X_{int} = \begin{bmatrix} -d_{cx} \cdot \cos(\alpha) + d_{cam} - d_{cz} \cdot \sin(\alpha) \\ -d_{cy} \\ -d_{cz} \cdot \cos(\alpha) + d_{cx} \cdot \sin(\alpha) \\ 0 \end{bmatrix} \quad (19)$$

All that remains now is to deduce the target to be reached. To do this, we need to take into account the fact that we are not trying to hit the target, but to get within a certain distance d_{obj} . We can now write down the objective as w :

$$w = \begin{bmatrix} -d_{obj} \cdot \cos(\alpha) + d_{cam} \\ 0 \\ d_{cx} \cdot \sin(\alpha) \\ -\text{err}_{\theta_h} \end{bmatrix} \quad (20)$$

The target is to keep the airship remain stationary in front of the target, so we have $\dot{w} = 0$ and $\ddot{w} = 0$. We then apply the principle of PID. We define the variable V :

$$V = (w - X_{int}) + 2 \times (\dot{w} - \dot{X}) + \ddot{x} = w - X_{int} - 2X \quad (21)$$

The coefficients (1, 2, 1) have been chosen arbitrarily and can be improved by experiment. We can then give the commands :

$$U = A^{-1} \cdot (V - B) \quad (22)$$

These commands are transmitted to the vrep_interm.py program by publisher ROS, which deduces the airship's evolution and updates its position. This control was only tested in simulation with arbitrary values for the parameters specific to the airship's dynamics, but the results obtained were satisfactory, with a decrease in error corresponding to what could be expected

6 PROGRESS MADE IN THE INTERNSHIP

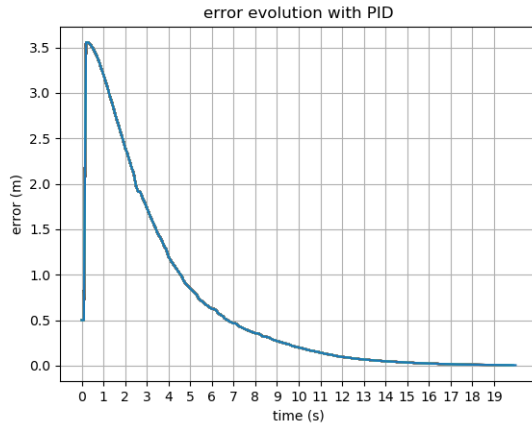


Figure 27: Distance error over time with control by PID.

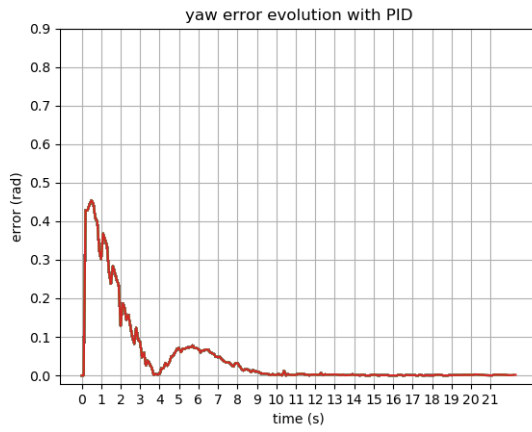


Figure 28: Course error over time with aPID controller.

with a coherent speed for this mini-blimp (Figs. 27 and 28, the start peaks correspond to the initialization of the system).

It should be noted that this control algorithm assumes that each motor can be controlled individually in a linear fashion. However, this is not currently the case: the airship's drivers have been written in such a way that the motors are controlled in an all-or-nothing manner, and the two lateral motors are controlled at the same time (translation along y is therefore not possible). This is a point to be corrected for a future job. In addition, we have just discovered that the lateral motors are not at the same distance from the robot's center of mass, so the torque is not correctly estimated. This problem is in the process of being solved, but it will probably be solved after the end of my contribution to the project.

6.4 Simulation

As the benefits of the smart camera could not be tested on the mini-blimp due to lack of time, I have instead created a simulation to carry out my control tests. To do this I used the v-rep software which has two advantages: firstly, it's free, and secondly, it can work with ROS. As I wanted to model the airship directly in the simulation, I created a cylinder to which I linked the visual of our airship obtained from Fusion360 and I defined its inertia matrix I as that of our mini airship.

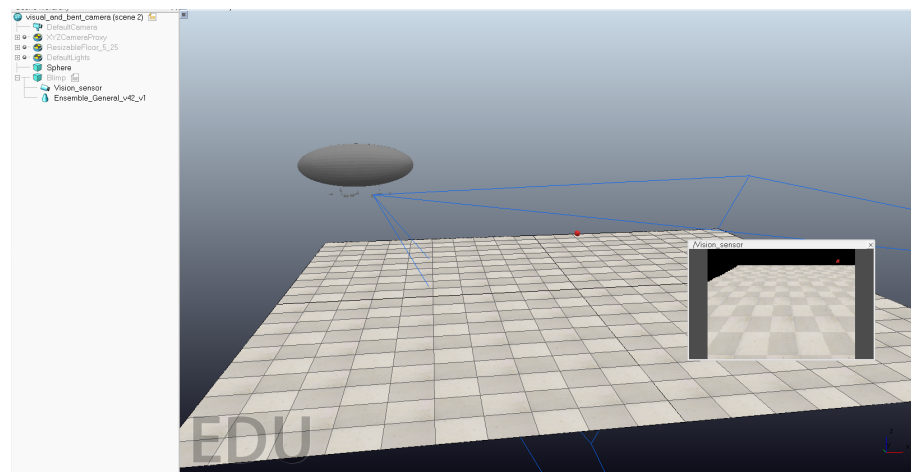


Figure 29: Simulation scene in v-rep.

However, the behavior obtained didn't seem to correspond to reality. What's more, the modelling of aerial drones in v-rep didn't seem to meet our expectations. In fact, I could only find one example of an aerial drone, which was one of the basic robots proposed. It was a quadcopter with four vertical motors that uses a particle projection system to calculate its thrust. Given the short time we had left, I decided to consider the airship as non-dynamic in v-rep and to control its position directly. I also added a camera to the airship and placed a red sphere in the scene with dimensions approaching those of a human head. The simulation camera has the same parameters as the Luxonis camera, particularly the aperture. The only difference is the resolution, which is of lower quality in the case of the simulation, because too high a resolution would lead to image processing taking too long and would therefore be impractical for real time. We now have a fairly simple scene (Fig. 29), but we still have to make the airship move.

To do this, I made the created scene communicate with a python program called `vrep_interm.py`, using ROS Noetic. This program retrieves the positions of the various objects in the scene and the camera image, as well as the motor commands sent by the control algorithm (Fig. 30). From this information, it uses the equations obtained by modelling the airship's dynamics to deduce its new position in the scene.

8 CONCLUSION

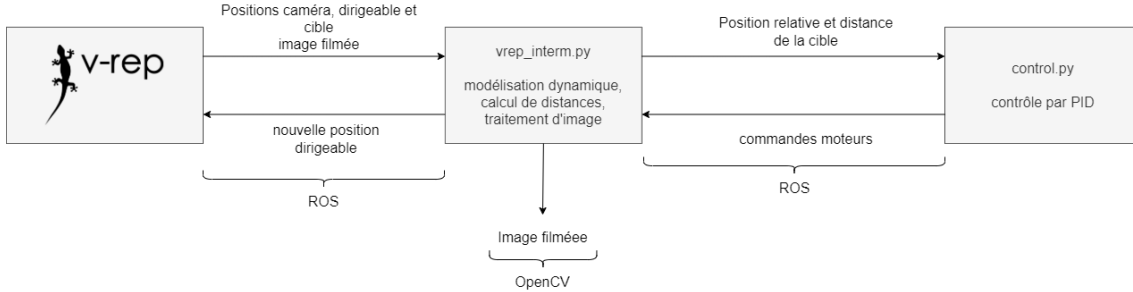


Figure 30: Simulation communication with ROS.

This program also does the work of the Luxonis camera: not only does it use the positions of the objects to deduce the distance from the target sphere to the camera, but it also performs image processing to deduce the position of the sphere in the camera's view. To do this, the image is converted to HSV format and the pixels whose H value corresponds to red are searched for, then their positions are averaged. This simplistic method can be applied because we are dealing here with a sphere, which is the only red object in the scene and has the advantage of being able to be performed in real time. Apart from the simulation, this work is carried out by the Luxonis, which is sufficiently powerful for this purpose. These two pieces of information are sent, again using ROS, to another control program, which only has access to the information that the Luxonis camera can provide.

7 Further steps and solutions

In these last days of my internship, my tasks will be finishing the documentation for next collaborators, so they can fix the problems we found in the current prototype, then improve and implement the control system we built.

If there is time left, my second task will be adapting the new envelope and the components in order to fly in a horizontal plane without any inclination in the pitch angle. This will lead to an even distribution of the forces and torques, which is essential for the automation of the blimp.

Besides the weight distribution, another big problem for the automation of the blimp is the difference between the senses of thrusters. Therefore, a major task for the next collaborators is the design of a new Li-Po SHIM system 19, as the main issue is the power given when the sense is inverted.

8 Conclusion

This report can be seen a summary of the work done during my internship in the project NOV-ABOT, an innovating project involving arts and science.

In this internship, I had the wonderful opportunity to discover how arts and engineering can have a space to be creative in both fields, and have my first approach to real robotics. Through this experience, I had the opportunity to apply most of the subjects I have seen through my studies, I hope I can work on the mechatronics' field later in my career.

While we were building the dynamic model, my mechatronics background was helpful since every test lead us to a new perturbation that had to be considered in the theoretical model, in the same way in the prototype we found flaws in the prototype that had to be fixed to fit the theoretical model. Thus after many flight tests, I learned that the theoretical model and real prototype are in constant change until both can behave as it is expected.

During the process of adapting the prototype to behave as the theoretical model, we faced many problems from previous designs because the goals of this stage were different from the past ones, thus they didn't notice there was an issue. This is a valuable lesson because now I will consider some extra time to analyze and fix past designs problems that haven't been noticed yet.

9 ACRONYMS

9 Acronyms

CNRS Centre National de la Recherche Scientifique

ISM Institut des Sciences du Mouvement - Etienne-Jules Marey (CNRS/Aix Marseille Université, ISM UMR7287)

LESA Laboratoire d'Etudes en Sciences des Arts (Aix Marseille Université, LESA EA 3274)

PID controller Proportional Integral Derivative

PD controller Proportional Derivative

ROS Robot Operating System

ID-Fab Innovation, Fabrication-Design

AMU Aix Marseille Université

SLAM Simultaneous Localisation And Mapping

UAV Unmanned Aerial Vehicle

LTAR Lighter Than Air Robot

Li-Po Lithium-Polymer

RGBD Red Green Blue Distance

GT-MAB Georgia Tech Miniature Autonomous Blimp

References

- [1] Alexander Borst. Models of motion detection. *Nature neuroscience*, 3(11):1168–1168, 2000.
- [2] Florent Boughanem. Conception mécanique d'un mini ballon dirigeable destiné au vol intérieur dans le cadre du projet novabot, June 2021.
- [3] Sungjin Cho, Vivek Mishra, Qiuyang Tao, Paul Varnell, Matt King-Smith, Aneri Muni, Weston Smallwood, and Fumin Zhang. Autopilot design for a class of miniature autonomous blimps. In *2017 IEEE conference on control technology and applications (CCTA)*, pages 841–846. IEEE, 2017.
- [4] Sungjin Cho, Qiuyang Tao, Paul Varnell, Sean Maxon, and Fumin Zhang. Autopilot design of a class of miniature autonomous blimps enabled by switched controllers. *International Journal of Intelligent Robotics and Applications*, 6(3):385–396, 2022.
- [5] Jürg Germann, Michael Dommer, Ramon Pericet-Camara, and Dario Floreano. Active connection mechanism for soft modular robots. *Advanced Robotics*, 26(7):785–798, 2012.
- [6] Pablo González, Wolfram Burgard, Rafael Sanz Domínguez, and Joaquín López Fernández. Developing a low-cost autonomous indoor blimp. 2009.
- [7] Marina González-Álvarez, Julien Dupeyroux, Federico Corradi, and Guido CHE De Croon. Evolved neuromorphic radar-based altitude controller for an autonomous open-source blimp. In *2022 International Conference on Robotics and Automation (ICRA)*, pages 85–90. IEEE, 2022.
- [8] Gal Gorjup and Minas Liarokapis. A low-cost, open-source, robotic airship for education and research. *IEEE Access*, 8:70713–70721, 2020.
- [9] Mengxue Hou, Qiuyang Tao, and Fumin Zhang. Human pointing motion during interaction with an autonomous blimp. *Scientific Reports*, 12(1):11402, 2022.
- [10] Fumiya Iida. Goal-directed navigation of an autonomous flying robot using biologically inspired cheap vision. In *Proceedings of the 32nd ISR (International Symposium on Robotics)*, volume 19, pages 21–27, 2001.
- [11] Fumiya Iida and Dimitrios Lambrinos. Navigation in an autonomous flying robot by using a biologically inspired visual odometer. In *Sensor fusion and decentralized control in robotic systems III*, volume 4196, pages 86–97. SPIE, 2000.
- [12] Daizo Ikeda. Blade-free drone. *NTT DOCOMO Tech J*, 21(4):37–43, 2020.
- [13] Youssra Mansar, François Bernier, Sylvain Blayac, Julien Serres, and Louis Dieuzayde. Novabot: Acteur et drone. dialectique du corps en scène et de son image fragmentée. In *Drôles d'objets-Un nouvel art de faire*, Nancy, France, 05 2023.

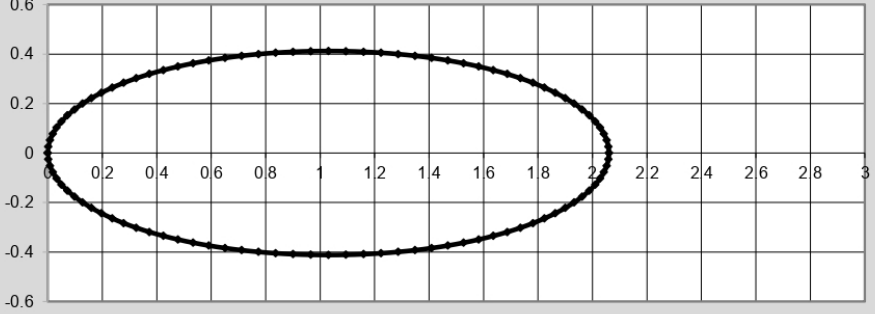
- [14] Nagamalar Nagarajan. *Multi-Objective Optimisation of RTAB-Map Parameters Using Genetic Algorithm for Indoor 2D SLAM*. PhD thesis, 2020.
- [15] Seungyong Oh, Sungchul Kang, Kyungjoon Lee, Sangchul Ahn, and Euntai Kim. Flying display: Autonomous blimp with real-time visual tracking and image projection. In *2006 IEEE/RSJ International Conference on Intelligent Robots and Systems*, pages 131–136. IEEE, 2006.
- [16] Yasuhiro Ohata, Satoshi Ushijima, and Dragomir N Nenchev. Development of an indoor blimp robot with internet-based teleoperation capability. In *Proc. 13th IASTED International Conference on Robotics and Applications*, pages 186–191, 2007.
- [17] Ho Shing Poon, Mark KK Lam, Maxwell Chow, and Wen J Li. Noiseless and vibration-free ionic propulsion technology for indoor surveillance blimps. In *2009 IEEE International Conference on Robotics and Automation*, pages 2891–2896. IEEE, 2009.
- [18] Michelle Rossouw. *An open-source autopilot and bio-inspired source localisation strategies for miniature blimps*. PhD thesis, UNSW, Canberra, 06 2023.
- [19] Landan Seguin, Justin Zheng, Alberto Li, Qiuyang Tao, and Fumin Zhang. A deep learning approach to localization for navigation on a miniature autonomous blimp. In *2020 IEEE 16th International Conference on Control & Automation (ICCA)*, pages 1130–1136. IEEE, 2020.
- [20] Julien Serres, Stéphane Viollet, and Franck Ruffier. Microdrones bio-inspirés - doter nos futurs robots aériens de l’agilité des insectes. *Les Techniques de l’Ingénieur*, pages S7717–V1, 2017.
- [21] Florian Siccardi. Novabot : un mini dirigeable dédié à la captation scénique, 2022.
- [22] P.B. Sujit, Srikanth Saripalli, and Joao Borges Sousa. Unmanned aerial vehicle path following: A survey and analysis of algorithms for fixed-wing unmanned aerial vehicles. *IEEE Control Systems Magazine*, 34(1):42–59, 2014.
- [23] Qiuyang Tao, Jaeseok Cha, Mengxue Hou, and Fumin Zhang. Parameter identification of blimp dynamics through swinging motion. In *2018 15th International Conference on Control, Automation, Robotics and Vision (ICARCV)*, pages 1186–1191. IEEE, 2018.
- [24] Qiuyang Tao, Mengxue Hou, and Fumin Zhang. Modeling and identification of coupled translational and rotational motion of underactuated indoor miniature autonomous blimps. In *2020 16th International Conference on Control, Automation, Robotics and Vision (ICARCV)*, pages 339–344. IEEE, 2020.
- [25] Qiuyang Tao, Tun Jian Tan, Jaeseok Cha, Ye Yuan, and Fumin Zhang. Modeling and control of swing oscillation of underactuated indoor miniature autonomous blimps. *Unmanned Systems*, 9(01):73–86, 2021.

- [26] Qiuyang Tao, Junkai Wang, Zheyuan Xu, Tony X Lin, Ye Yuan, and Fumin Zhang. Swing-reducing flight control system for an underactuated indoor miniature autonomous blimp. *IEEE/ASME Transactions on Mechatronics*, 26(4):1895–1904, 2021.
- [27] Hiroaki Tobita. Augmented reality system. *US Patent 9779550B2*, 2017.
- [28] Paul Viola and Michael J Jones. Robust real-time face detection. *International journal of computer vision*, 57:137–154, 2004.
- [29] Yue Wang, Gang Zheng, Denis Efimov, and Wilfrid Perruquetti. Disturbance compensation based controller for an indoor blimp robot. *Robotics and Autonomous Systems*, 124:103402, 2020.
- [30] Ning-shi Yao, Qiu-yang Tao, Wei-yu Liu, Zhen Liu, Ye Tian, Pei-yu Wang, Timothy Li, and Fumin Zhang. Autonomous flying blimp interaction with human in an indoor space. *Frontiers of Information Technology & Electronic Engineering*, 20(1):45–59, 2019.
- [31] Ningshi Yao, Emily Anaya, Qiuyang Tao, Sungjin Cho, Hongrui Zheng, and Fumin Zhang. Monocular vision-based human following on miniature robotic blimp. In *2017 IEEE International Conference on Robotics and Automation (ICRA)*, pages 3244–3249. IEEE, 2017.
- [32] Fumin Zhang, Qiuyang Tao, Tun Jian Tan, Chengn Phillip Sung Tse, Sungjin Cho, Vivek Mishra, and Jesse P. Varnell. Miniature autonomous robotic blimp, 2019. US Patent 0258257A1.
- [33] Jean-Christophe Zufferey. *Bio-inspired vision-based flying robots*. PhD thesis, EPFL, 2005.
- [34] Jean-Christophe Zufferey, Alexis Guanella, Antoine Beyeler, and Dario Floreano. Flying over the reality gap: From simulated to real indoor airships. *Autonomous Robots*, 21:243–254, 2006.

REFERENCES

Appendices

REFERENCES

Airship Envelope Datasheet			
Identifier:	Faculté des sciences du sport	Date of Design:	2023-04-18
Designed by:	Dr Julien Serres	Date of Production:	
Organisation:		Place of Production:	Windreiter HQ
			
Material Parameter		Gertler Shape Coefficients	
Envelope Material:	TritaX Silver	Position of max. thickness:	0.5
Surface Weight [g/m²]:	30	Bow Radius:	0.5
Tension Strength [MPa]:	245	Stern Radius:	0.5
Bonding Technique:	Point Welding	Prismatic Coefficient:	0.67
Design Parameter		Lift Assumptions*	
Length to Diameter:	2.500	Lift at Sea Level He [g]:	600.40
Block Volume [m³]:	1.400	Lift at 300 m Helium [g]:	578.41
Block Coefficient:	0.526	Lift at Sea Level H2 [g]:	647.01
Envelope Volume [l]:	736.70	Lift at 300 m H2 [g]:	623.31
Length [m]:	2.06	*The calculations assume pure lifting gas	
Diameter [m]:	0.82		
Surface Area [m²]:	4.54		
Envelope Weight [g]:	136.30		
Number of gores	4		

Gertler 4621 Shape spreadsheet. Computes shape, volume, centre of volume, and pattern for a Series58 Model 4621 body of revolution. Copyright (C) 2019 Johannes Eissing

Customized Envelope Production Services by the Windreiter Team
 Single envelopes to large numbers

www.windreiter.de